

# The structure and energetics of $^3\text{He}$ and $^4\text{He}$ nanodroplets doped with alkaline earth atoms

Alberto Hernando, Ricardo Mayol, Martí Pi, and Manuel Barranco  
*Departament ECM, Facultat de Física, and IN<sup>2</sup>UB,  
Universitat de Barcelona. Diagonal 647, 08028 Barcelona, Spain*

Francesco Ancilotto  
*INFN-DEMOCRITOS and Dipartimento di Fisica 'G. Galilei',  
Università di Padova, via Marzolo 8, I-35131 Padova, Italy*

Oliver Bünermann and Frank Stienkemeier  
*Physikalisches Institut, Universität Freiburg.  
Hermann-Herder-Str. 3, D-76104 Freiburg, Germany*

## Abstract

We present systematic results, based on density functional calculations, for the structure and energetics of  $^3\text{He}$  and  $^4\text{He}$  nanodroplets doped with alkaline earth atoms. We predict that alkaline earth atoms from Mg to Ba go to the center of  $^3\text{He}$  drops, whereas Ca, Sr, and Ba reside in a deep dimple at the surface of  $^4\text{He}$  drops, and Mg is at their center. For Ca and Sr, the structure of the dimples is shown to be very sensitive to the He-alkaline earth pair potentials used in the calculations. The  $5s5p \leftarrow 5s^2$  transition of strontium atoms attached to helium nanodroplets of either isotope has been probed in absorption experiments. The spectra show that strontium is solvated inside  $^3\text{He}$  nanodroplets, supporting the calculations. In the light of our findings, we emphasize the relevance of the heavier alkaline earth atoms for analyzing mixed  $^3\text{He}$ - $^4\text{He}$  nanodroplets, and in particular, we suggest their use to experimentally probe the  $^3\text{He}$ - $^4\text{He}$  interface.

Keywords: atomic clusters, visible spectroscopy, density functional theory.

## I. INTRODUCTION

Optical investigations of impurities in liquid helium have drawn considerable attention in the past.<sup>1</sup> In recent years, experiments involving helium nanodroplets have added new input into the interaction of atomic impurities with a superfluid helium environment.<sup>2,3</sup> In particular, the shifts of the electronic transition lines represent a very useful observable to determine the location of the foreign atom attached to a helium drop.

While most impurities are found to reside in the interior of helium droplets,<sup>4,5,6,7</sup> it is well-established that alkali atoms, due to their weak interaction with helium, reside in a ‘dimple’ at the surface of the drop for both helium isotopes.<sup>8,9,10</sup> The question of solvation versus surface location for an impurity atom in liquid He can be addressed within the model of Ref. 11, where a simple criterion has been proposed to decide whether surface or solvated states are energetically favored. An adimensional parameter  $\lambda$  can be defined in terms of the impurity-He potential well depth  $\epsilon$  and the minimum position  $r_{min}$ , namely,  $\lambda \equiv \rho \epsilon r_{min} / (2^{1/6} \sigma)$ , where  $\rho$  and  $\sigma$  are the density and surface tension of bulk liquid He, respectively. The threshold for solvation in  $^4\text{He}$  is<sup>11</sup>  $\lambda \sim \lambda_0$ , with  $\lambda_0 = 1.9$ . When  $\lambda < \lambda_0$ , a stable state of the impurity on the droplet surface is expected, whereas when  $\lambda > \lambda_0$ , the impurity is likely to be solvated in the interior of the droplet. Impurities such as neutral alkali atoms, that weakly interact with helium, are characterized by values of  $\lambda$  much smaller than the above threshold; their stable state is thus expected to be on the surface of the droplet, as experimentally found.

The shape of the impurity-He interaction potential, however, is not given consideration by this model. For cases in which the value of  $\lambda$  does not lie near (say, within 0.5) the solvation threshold  $\lambda_0$ , the shape of the potential surface does not need to be taken into account, as the model is predictive outside of this threshold window. However, for values which lie close to  $\lambda_0$ , consideration of the shape of the potential energy surface, as well as the well depth and equilibrium internuclear distance, is mandatory, and more detailed calculations are needed to ascertain whether the impurity is solvated or not. It is worth noticing that the above criterion works for either helium isotope, although so far, it has been applied to  $^4\text{He}$  because experimental data for  $^3\text{He}$  only appeared recently.<sup>8,12,13,14</sup>

Among simple atomic impurities, alkaline earth (Ake) atoms play a unique role. While, for example, all alkali atoms reside on the surface and all noble gas atoms reside in the

interior of drops made of either isotope,<sup>15</sup> the absorption spectra of heavy alkaline earth atoms Ca, Sr, and Ba attached to a  $^4\text{He}$  cluster clearly support an outside location of Ca and Sr<sup>16</sup> and likely also of Ba,<sup>17</sup> whereas for the lighter Mg atom, the experimental evidence shows that it resides in the interior of the  $^4\text{He}$  droplets.<sup>18,19</sup>

According to the magnitude of the observed shifts, the dimple in the case of alkaline earth atoms is thought to be more pronounced than in the case of alkalis, indicating that alkaline earth atoms reside deeper inside the drop than alkali atoms. This will be corroborated by density functional calculations presented in the Theoretical Results. Laser-induced fluorescence results for Ca atoms in liquid  $^3\text{He}$  and  $^4\text{He}$  have been recently reported<sup>20</sup> and have been analyzed using a vibrating ‘bubble model’ and fairly old Ca-He pair potentials based on pseudopotential SCF/ CI calculations.<sup>21</sup>

Applying the simple criterion described above, Ca and Sr appear to be barely stable in their surface location with respect to the bulk one,<sup>22</sup> as reflected in the  $\lambda$  values collected in Table I, which are close to  $\lambda_0$  for these doped  $^4\text{He}$  systems. This borderline character for the solvation properties of these impurities implies that detailed calculations are required to help to understand the results of spectroscopic studies on alkalineearth- doped He droplets. In particular, high-quality impurity- He pair interaction potentials are required since even relatively small inaccuracies in these potentials, which are often not known with a sufficient precision, may yield wrong results.

We present here a systematic study for helium drops made of each isotope, having a number of atoms large enough to make them useful for the discussion of experiments on laser-induced fluorescence (LIF) or beam depletion (BD) spectroscopy or for the discussion of other physical phenomena involving these systems, such as interatomic Coulombic decay.<sup>23,24</sup> We also discuss the dependence of the structural properties on the cluster size. Some of this information is also experimentally available.<sup>17</sup> After a brief explanation of the experiment, results are presented for strontium on helium nanodroplets that further support the calculations.

This work is organized as follows. In Sec. II we briefly describe the density functional plus alkaline earth-He potential approach employed here, as well as some technical details. Doped drops calculations are presented and discussed in Sec. III, while the experimental results are discussed in Sec. IV, and an outlook is presented in Sec. V.

## II. DENSITY-FUNCTIONAL DESCRIPTION OF HELIUM NANODROPLETS

Since the pioneering work of Stringari and coworkers,<sup>25</sup> density functional (DF) theory has been used in many studies on liquid helium in confined geometries and found to provide a quite accurate description of the properties of inhomogeneous liquid He (see e.g. Ref. 15 and references therein).

The starting point is to write the energy of the system as a functional of the He particle density  $\rho$ :

$$E[\rho] = \int d\mathbf{r} \mathcal{E}(\rho) + \int d\mathbf{r}' \rho(\mathbf{r}') V_{Ake-He}(|\mathbf{r} - \mathbf{r}'|), \quad (1)$$

where  $\mathcal{E}(\rho)$  is the He energy density per unit volume, and  $V_{Ake-He}$  is the alkaline earth-helium pair potential. The impurity is thus treated as a fixed external potential. Addressing the lightest alkaline earth, Be, for which a fairly recent Be-He is available,<sup>26</sup> would likely require to treat this atom as a quantum particle instead of as an external potential.<sup>15</sup>

For  $^4\text{He}$  we have used the Orsay-Trento functional,<sup>27</sup> and for  $^3\text{He}$  the one described in Ref. 28 and references therein. These functionals have been used in our previous work on helium drops doped with alkali atoms<sup>8,9</sup> as well as in many other theoretical works. The results discussed in the following have been mostly obtained using the potentials of Ref. 29 (Ca, Sr and Ba), and of Ref. 30 (Mg, for which the pair potentials of Refs. 26 and 30 are similar). For Ca, we have also tested other potentials available in the literature,<sup>26,30,31</sup> as well as the unpublished potential of Meyer<sup>32</sup> we had employed in our previous work.<sup>22</sup>

Fig. 1 shows the pair potentials used in this work. From this figure, one may anticipate that  $\text{Ca}@^4\text{He}_N$  drops described using the potential of Ref. 32 display deeper dimples than the same drops described with the potential of Ref. 29. We want to point out that the Ca-He potentials of Refs. 26 and 30 are very similar to that of Ref. 29, and should yield equivalent results. Contrarily, we have found that the potential of Ref. 31 is more attractive, causing the Ca atom to be drawn to the center of the  $^4\text{He}_N$  drop, in contrast with the experimental findings.<sup>17</sup>

For a number  $N$  of helium atoms in the drop, we have solved the Euler-Lagrange equation which results from the variation of  $E[\rho]$  at constant  $N$ :

$$\frac{\delta \mathcal{E}}{\delta \rho} + V_{Ake-He} = \mu, \quad (2)$$

where  $\mu$  is the helium chemical potential, whose value is determined self-consistently by

imposing the auxiliary condition  $\int d\mathbf{r}\rho(\mathbf{r}) = N$  during the iterative minimization.

When the impurity resides off center (as in the case of a dimple structure), the system is axially symmetric. Despite this symmetry, we have solved Eq. (2)

in Cartesian coordinates because this allows us to use fast Fourier transform techniques<sup>33</sup> to efficiently compute the convolution integrals entering the definition of  $\mathcal{E}(\rho)$ , that is, the mean field helium potential and the coarse-grained density needed to evaluate the correlation term in the density functional.<sup>27</sup> We have found this procedure to be faster and more accurate than convoluting by direct integration using cylindrical coordinates.

We have used an imaginary time method<sup>34,35</sup> to solve Eq. (2), after having discretized it using 13-point formulas for the spatial derivatives. The mesh used to discretize  $\rho$  in space is chosen so that the results are stable against small changes of the mesh step.

### III. THEORETICAL RESULTS

We start a typical calculation by placing the impurity close to the surface of the He droplet. Depending on the studied impurity and/or the He isotope, during the functional minimization, the alkaline earth atom is either driven to the interior of the droplet,<sup>36</sup> or it remains trapped in a more or less pronounced dimple on its surface.

In the case of  ${}^3\text{He}$ , we find that for all of the alkaline earth atoms investigated, the stable state is always the one where the impurity is in the center of the cluster. This is consistent with the associated large  $\lambda$  values, see Table I. Figure 2 shows the density profiles for  $\text{Mg}@{}^3\text{He}_N$ ,  $\text{Ca}@{}^3\text{He}_N$ ,  $\text{Sr}@{}^3\text{He}_N$ , and  $\text{Ba}@{}^3\text{He}_N$  for  $N = 300, 500, 1000, 2000, 3000$ , and  $5000$ . For  $\text{Ca}@{}^3\text{He}_{5000}$ , we also show the profile obtained with the pair potential of Ref. 32 (dotted line). Several solvation shells are clearly visible. The number of  ${}^3\text{He}$  atoms below the first solvation peak for the  $N = 5000$  drop is about 19 for Mg, 22 for Ca, 26 for Sr, and 27 for Ba. The differences in the location and height of the first solvation peak are a simple consequence of the different depth and equilibrium distance of the corresponding pair potentials. It is interesting to see the building up of the drop structure around the impurity that, as it is wellknown,<sup>5</sup> only causes a large but localized effect on the drop structure.

The bottom panel of Fig. 3 shows the corresponding solvation energies, defined as the energy differences

$$S_N(Ake) = E(Ake@{}^3\text{He}_N) - E({}^3\text{He}_N), \quad (3)$$

with an equivalent definition for  $^4\text{He}$  drops. The more attractive Ca-He pair potential of Ref. 32 yields, on average, a solvation energy about 13 K larger as compared with that obtained with the pair potential of Ref. 29, despite the fact that the density profiles look fairly similar; see Fig. 2.

In the case of Ca and Sr atoms in  $^4\text{He}$  drops, whose  $\lambda$  values are close to the threshold for solvation  $\lambda_0$  (see Table I), we have found that, for both dopants, the minimum energy configuration is a dimple state at the surface, although the energy difference between the surface and the solvated states is fairly small for both dopants. For  $\text{Ca}@^4\text{He}_{300}$ , this difference is 3.4 K using Meyer's potential,<sup>22</sup> and 12.0 K using that of Ref. 29. The homologous result for  $\text{Sr}@^4\text{He}_{300}$  is 22.7 K. These energy differences have to be compared with the total energy of the  $^4\text{He}_{300}$  drop, which is about  $-1384$  K.

We have also confirmed by DF calculations the surface state of  $\text{Ba}@^4\text{He}_N$  and the solvated state of  $\text{Mg}@^4\text{He}_N$ , both suggested by the corresponding  $\lambda$  values in Table I. This is illustrated in Fig. 4 for Mg, and in Fig. 5 for Ca, Sr and Ba. The dimple depth  $\xi$ , defined as the difference between the position of the dividing surface at  $\rho = \rho_b/2$  -where  $\rho_b$  is the bulk liquid density- with and without impurity, respectively, is shown in Fig. 6 as a function of  $N$ . The structure of the dimple is different for different alkaline earth atoms, being shallower for Ba and more pronounced for Ca. We recall that the  $\xi$  values for  $\text{Na}@^3\text{He}_{2000}$  and  $\text{Na}@^4\text{He}_{2000}$  are 4.5 and 2.1 Å, respectively.<sup>8</sup> The dimple depths for alkaline are thus much smaller than for alkaline earth atoms, as also indicated by LIF experiments.<sup>2,8,16,17</sup> The dependence of the the dimple depth with the alkaline earth atom size, characterized by the radial expectation value  $R_{Ake}$  of the valence electrons,<sup>37</sup> is shown in Fig. 7. This figure is consistent with the increasing bulk-to-surface ratio of the line shifts as the size of the dopant atom increases.<sup>17</sup>

The 'solvation' energies for these alkaline earth atoms in  $^4\text{He}$  drops are displayed in the top panel of Fig. 3. As in the case of  $^3\text{He}$  drops discussed before, the stronger the Ake-He pair potential (see Fig. 1), the more negative  $S_N(\text{Ake})$ . In the case of  $\text{Ca}@^4\text{He}_N$  and  $\text{Sr}@^4\text{He}_N$ , the energies are very similar, and so are the dimple depths shown in Fig. 6. It is worth seeing the different behavior of  $S_N$  as a function of  $N$  for each helium isotope. In the case of  $^3\text{He}$ , once the first 2-3 solvation shells are fully developed,  $S_N$  quickly saturates, and for this reason it changes only by 12 % (Ca) and 17 % (Sr) from  $N = 300$  to  $N = 5000$ . For the same reason, spectroscopic shifts are expected to be  $N$  independent for drops made of

more than a few hundred  $^3\text{He}$  atoms. When the impurity is at the surface, sizeable curvature effects appear even for a few thousand atoms drops. This shows up not only in the change of  $S_N$ , which is about 22 % for Ca, and 24 % for Sr in the same  $N$  range as before, but also in the spectroscopic shifts, that still depend on  $N$  below  $N \sim 3000$  (see e.g. Ref. 17). This illustrates the need of large drops for carrying out spectroscopic shift calculations to attempt a detailed comparison with experiments.

#### IV. EXPERIMENTAL RESULTS

To support the DF calculations, the  $5s5p\ ^1P_1^o \leftarrow 5s^2\ ^1S_0$  transition of strontium on nanodroplets made of either helium isotope has been experimentally investigated. Although calcium appears to be most favorable, we are so far restricted to excitation spectra of strontium attached to helium droplets because of the limited tuning range of our lasers. Calcium will be addressed in a future experiment. The experiments were performed in a helium droplet machine applying laser-induced fluorescence, as well as beam depletion and photoionization (PI) spectroscopy. A detailed description of the experimental setup is presented elsewhere.<sup>17</sup> Modifications include a new droplet source to reach the lower temperatures needed for generating  $^3\text{He}$  droplets.<sup>8</sup> In short, gas of either helium isotope is expanded under supersonic conditions from a nozzle, forming a beam of droplets traveling freely in high vacuum. The helium stagnation pressure in the droplet source is 20 bar, and a nozzle of  $5\ \mu\text{m}$  diameter has been used. The nozzle temperature has been stabilized to 12 K and 15 K to form  $^3\text{He}$  and  $^4\text{He}$  droplets, respectively. These conditions result in an average droplet size of  $\sim 5000$  helium atoms.<sup>7</sup>

The droplets are doped downstream using the pick-up technique: in a heated scattering cell, an appropriate vapor pressure of strontium is established so that droplets pick up one single atom on average when passing the cell. LIF as well as PI and BD absorption spectra of the doped droplet beam can be recorded upon electronic excitation using a pulsed nanosecond dye laser. LIF is recorded with a photo multiplier tube. In the case of PI, the photons of an excimer laser ionize the excited atoms in a one photon step. The ions are afterwards detected by a channeltron. For the beam depletion measurement, a Langmuir-Taylor surface ionization detector has been used.<sup>38</sup>

We show here only the results obtained using LIF because a much better signal-to-noise

ratio was achieved when compared to the PI and BD spectra for strontium doped clusters. In the case of PI, the reason probably is the tendency of the just formed strontium ions not to desorb from the droplet like e.g. alkali atoms do. Since the detection efficiency of our PI detector is considerably decreased for high masses, the detection of the ion+droplet complex is small. A decreased desorption mechanism also diminishes the sensitivity of BD techniques. However, the PI/BD measurements give identical results when compared to the LIF spectra.

Figure 8 shows the measured spectra of the  $5s5p\ ^1P_1^o \leftarrow 5s^2\ ^1S_0$  transition of strontium atoms on droplets of  $^3\text{He}/^4\text{He}$  compared to that in bulk  $^4\text{He}$ .<sup>39</sup> All three spectra show a broad asymmetric line, blue shifted from the atomic gas-phase absorption. The differences of the shifts for  $^4\text{He}$  drops and bulk  $^4\text{He}$  immediately confirms the surface location of the strontium atoms.<sup>16</sup> In the case of bulk  $^4\text{He}$ , the absorption is far more blue shifted and the width is considerably wider. The shift can be explained within the bubble model, see e.g. Refs. 1,20 and references therein, and results from repulsion of the helium environment against spatial enlargement of the electronic distribution of the excited state. The shift in bulk helium is larger than in droplets because the dopant is completely surrounded by helium, whereas it is not when it is located at the surface of drops.

Table II summarizes the experimentally determined shifts of the first electronic transition of strontium and calcium in helium droplets, as well as the measurements in bulk helium for both isotopes. As compared to  $^4\text{He}$  drops, the absorption maximum in the case of  $^3\text{He}$  drops is shifted  $60\text{ cm}^{-1}$  further to the blue, and the width increases from  $180$  to  $220\text{ cm}^{-1}$ .

At first glance, it is not obvious from the recorded spectra in  $^3\text{He}$  drops whether the strontium atom is in a surface state, or it is solvated inside the droplets. It is worth mentioning that Morowaki et al. performed similar measurements in bulk helium.<sup>20</sup> They have compared the absorption spectra of the  $4s4p\ ^1P_1^o \leftarrow 4s^2\ ^1S_0$  transition of calcium in bulk  $^3\text{He}$  and  $^4\text{He}$ , and have found a much smaller blue shift in the case of  $^3\text{He}$  (about 55%, see Table II), which could again be explained within the bubble model -the reduced shift just results from the lower density of liquid  $^3\text{He}$ . A similar quantitative effect should be expected for strontium, especially in view of the reported DF calculations.

Consistent with this expectation is that in our experiments, the measured shift of Sr in  $^3\text{He}$  droplets,  $140\text{ cm}^{-1}$ , is about a 58% of the value corresponding to Sr in bulk  $^4\text{He}$ ,  $240\text{ cm}^{-1}$ .<sup>39</sup> We can safely argue that the shift determined in  $^3\text{He}$  droplets should sensibly



coincide with the expected value for bulk  $^3\text{He}$ , indicating complete solvation of strontium atoms in  $^3\text{He}$  droplets, as predicted by DF calculations.

## V. SUMMARY AND OUTLOOK

In this work, we have presented detailed results for the structure and energetics of helium drops doped with Mg, Ca, Sr, and Ba alkaline earth atoms. We have found that these atoms are solvated in the case of  $^3\text{He}$  drops and reside in surface dimples in the case of  $^4\text{He}$  drops, with the sole exception of  $\text{Mg}@^4\text{He}_N$ , which is also solvated. This yields a fairly complete physical picture, from the theoretical viewpoint, of the structure and energetics of helium drops doped with alkaline earth atoms. The experimental spectrum of strontium atoms in  $^4\text{He}$  and  $^3\text{He}$  droplets confirms the DF calculations. Moreover, since the spectroscopic shift is sensitive to the shape/depth of the surface dimple, a comparison between experimental and calculated line shifts could provide a sensible test on the accuracy of available pair potentials. We want to stress again that accurate pair potentials are needed to quantitatively reproduce the experimental results, especially when the solvation properties of the impurity are such that they yield values of  $\lambda$  close to the threshold value  $\lambda_0$ .

The different solvation behavior of the heavier alkaline earth atoms in  $^3\text{He}$  and  $^4\text{He}$  drops, offers the unique possibility of using them to study mixed drops at very low temperatures, in particular the  $^3\text{He}$ - $^4\text{He}$  interface. It is known that below the tricritical point at  $\sim 0.87\text{ K}$ ,<sup>40</sup>  $^3\text{He}$  has a limited solubility in  $^4\text{He}$ , segregating for concentrations larger than a critical value. This segregation also appears in mixed droplets,<sup>12,41,42</sup> producing a shell structure in which a core, essentially made of  $^4\text{He}$  atoms, is coated by  $^3\text{He}$  that is hardly dissolved into the  $^4\text{He}$  core, even when the number of  $^3\text{He}$  atoms is very large.<sup>41</sup> Due to this particular structure, that pertains to medium to large size droplets, strongly attractive impurities reside in the  $^4\text{He}$  core, being very little affected by the outer  $^3\text{He}$  shell, whereas weakly attractive impurities, like alkali atoms, should still reside in the surface of the droplet, irrespective of the existence of the  $^4\text{He}$  core. Contrarily, Ca, Sr and Ba impurities would be sunk into the fermionic component up to reaching the  $^3\text{He}$ - $^4\text{He}$  interface if the appropriate number of atoms of each isotope is chosen. This will offer the possibility of studying the  $^3\text{He}$ - $^4\text{He}$  interface, and a richer alkaline earth atom environment. We are at present generalizing the DF approach we have used in the past<sup>41</sup> to address this more demanding and promising new

aspect of the physics of doped helium droplets. On the experimental side, calcium spectra will be accessible in forthcoming experiments. We want to point out that mixed droplets doped with alkali atoms have been already detected in our previous experiments,<sup>14</sup> and that systematic experiments on alkaline earth doped mixed droplets will be performed in the future.

### Acknowledgments

We would like to thank Josef Tiggesbäumker and Marek Krośnicki for useful correspondence. This work has been performed under Grant No. FIS2005-01414 from DGI, Spain (FEDER), Grant 2005SGR00343 from Generalitat de Catalunya, and under the HPC-EUROPA project (RII3-CT-2003-506079), with the support of the European Community - Research Infrastructure Action under the FP6 'Structuring the European Research Area' Programme.

- 
- <sup>1</sup> Tabbert, B.; Günther, H.; zu Putlitz, G. *J. Low Temp. Phys.* **1997**, *109*, 653.
  - <sup>2</sup> Stienkemeier, F.; Vilesov, A. F. *J. Chem. Phys.* **2001**, *115*, 10119.
  - <sup>3</sup> Stienkemeier, F.; Lehmann, K. K. *J. Phys. B* **2006**, *39*, R127.
  - <sup>4</sup> Barnett, R. N.; Whaley, K. B. *Phys. Rev. A* **1993**, *47*, 4082.
  - <sup>5</sup> Dalfovo, F. *Z. Phys. D* **1994**, *29*, 61.
  - <sup>6</sup> Callegari, C.; Lehmann, K. K.; Schmied, R.; Scoles, G. *J. Chem. Phys.* **2001**, *115*, 10090.
  - <sup>7</sup> Toennies, J. P.; Vilesov, A. F. *Angew. Chem. Ind. Ed.* **2004**, *43*, 2622.
  - <sup>8</sup> Stienkemeier, F.; Bünermann, O.; Mayol, R.; Ancilotto, F.; Barranco, M.; Pi, M. *Phys. Rev. B* **2004**, *70* 214509.
  - <sup>9</sup> Mayol, R.; Ancilotto, F.; Barranco, M.; Pi, M.; Bünermann, O.; Stienkemeier, F. *J. Low Temp. Phys.* **2005**, *138*, 229.
  - <sup>10</sup> Ancilotto, F.; Cheng, E.; Cole, M. W.; Toigo, F. *Z. Phys. B: Condens. Matter* **1995**, *98*, 323.
  - <sup>11</sup> Ancilotto, F.; Lerner, P. B.; Cole, M. W. *J. Low Temp. Phys.* **1995**, *101*, 1123.
  - <sup>12</sup> Grebenev, S.; Toennies, J. P.; Vilesov, A. F. *Science* **1998**, *279*, 2083.
  - <sup>13</sup> Harms, J.; Toennies, J. P.; Barranco, M.; Pi, M. *Phys. Rev. B* **2001**, *63*, 184513.

- <sup>14</sup> Bünermann, O. Ph.D. Thesis, University of Bielefeld, Germany, 2006.
- <sup>15</sup> Barranco, M.; Guardiola, R.; Hernández, S.; Mayol, R.; Pi, M. *J. Low Temp. Phys.* **2006**, *142*, 1.
- <sup>16</sup> Stienkemeier, F.; Meier, F.; Lutz, H. O. *J. Chem. Phys.* **1997**, *107*, 10816.
- <sup>17</sup> Stienkemeier, F.; Meier, F.; Lutz, H. O. *Eur. Phys. J. D* **1999**, *9*, 313.
- <sup>18</sup> Reho, J.; Merker, U.; Radcliff, M. R.; Lehmann, K. K.; Scoles, G. *J. Chem. Phys.* **2000**, *112*, 8409.
- <sup>19</sup> Przystawik, A. Ph.D. Thesis, University of Rostock, Germany, 2007.
- <sup>20</sup> Moriwaki, Y; Morita, N. *Eur. Phys. J. D* **2005**, *33*, 323.
- <sup>21</sup> Czuchaj, E.; Rebentrost, F.; Stoll, H.; Preuss, H. *Chem. Phys. Lett.* **1991**, *182*, 191.
- <sup>22</sup> Ancilotto, F.; Barranco, M.; Pi, M. *Phys. Rev. Lett.* **2003**, *91*, 105302.
- <sup>23</sup> Cederbaum, L. S.; Zobeley, J.; Tarantelli, F. *Phys. Rev. Lett.* **1997**, *79*, 4778.
- <sup>24</sup> Kryzhevoi, N. V.; Averbukh, V.; Cederbaum, L. S. submitted to *Phys. Rev. Lett.* **2006**.
- <sup>25</sup> Stringari, S.; Treiner, J. *J. Chem. Phys.* **1987**, *87*, 5021.
- <sup>26</sup> Partridge, H.; Stallcop, J. R.; Levin, E. *J. Chem. Phys.* **2001**, *115*, 6471.
- <sup>27</sup> Dalfovo, F.; Lastri, A.; Pricauptenko, L.; Stringari, S.; Treiner, J. *Phys. Rev. B* **1995**, *52*, 1193.
- <sup>28</sup> Mayol, R.; Pi, M.; Barranco, M.; Dalfovo, F. *Phys. Rev. Lett.* **2001**, *87*, 145301.
- <sup>29</sup> Lovallo, C. C.; Klobukowski, M.; *J. Chem. Phys.* **2004**, *120*, 246.
- <sup>30</sup> Hinde, R. J. *J. Phys. B: At. Mol. Opt. Phys.* **2003**, *36*, 3119.
- <sup>31</sup> Czuchaj, E.; Krośnicki, M.; Stoll, H.; *Chem. Phys.* **2003**, *292*, 101.
- <sup>32</sup> Meyer, W. personal communication.
- <sup>33</sup> Frigo M.; Johnson, S. G. Proceedings of the IEEE. *The Design and Implementation of FFTW3*; 2005; 93(2), p 216.
- <sup>34</sup> Press, W. H.; Teulosky, S. A.; Vetterling, W. T.; Flannery, B. P. Numerical Recipes in Fortran 77: The Art of Scientific Computing; Cambridge University Press: Cambridge, 1999.
- <sup>35</sup> Ancilotto, F.; Austing, D. G.; Barranco, M.; Mayol, R.; Muraki, K.; Pi, M.; Sasaki, S.; Tarucha, S. *Phys. Rev. B* **2003**, *67*, 205311.
- <sup>36</sup> Since we treat the impurity as an infinitely heavy particle, what actually occurs is that during the functional minimization, helium is drawn towards the impurity, embedding it until a final, lowest energy configuration is reached where the impurity sits in the center of the droplet. Numerically, the process is optimized by computing the force acting on the impurity, and

moving it in the direction of that force, see e.g. Ref. 10.

- <sup>37</sup> Desclaux, J. P.; *At. Data Nucl. Data Tables* **1973**, *12*(4), 311.
- <sup>38</sup> Stienkemeier, F.; Wewer, M.; Meier, F.; Lutz, H. O.; *Rev. Sci. Instrum.* **2000**, *71*, 3480.
- <sup>39</sup> Bauer, H.; Beau, M.; Friedel, B.; Marchand, C.; Miltner, K. *Phys. Lett. A* **1990**, *146*, 134.
- <sup>40</sup> Edwards, D. O.; Pettersen, M. S. *J. Low Temp. Phys.* **1992**, *87*, 473.
- <sup>41</sup> Pi, M.; Mayol, R.; Barranco, M.; *Phys. Rev. Lett.* **1999**, *82*, 3093.
- <sup>42</sup> Fantoni, S.; Guardiola, R.; Navarro, J.; Zucker, A. *J. Chem. Phys.* **2005**, *123*, 054503.

TABLE I:  $\lambda$  parameter for the alkaline earth atoms and pair potentials used in this work.

	$\lambda$	
	$^3\text{He}$	$^4\text{He}$
Mg <sup>a</sup>	4.73	2.60
Ca <sup>a</sup>	3.78	2.08
Ca <sup>b</sup>	3.71	2.04
Ca <sup>c</sup>	4.02	2.21
Ca <sup>d</sup>	4.52	2.49
Sr <sup>b</sup>	3.48	1.92
Ba <sup>b</sup>	3.15	1.73

<sup>a</sup> Ref. 30. <sup>b</sup> Ref. 29. <sup>c</sup> Ref. 32. <sup>d</sup> Ref. 31.

TABLE II: Experimental shifts of the first electronic transition of Ca and Sr atoms in bulk helium as well as in drops. The values for Sr@He<sub>N</sub> are from this work. Previous experiments, carried out only for Sr@<sup>4</sup>He<sub>N</sub>, showed the same shifts.<sup>17</sup>

	bulk		drop	
	$^4\text{He}$	$^3\text{He}$	$^4\text{He}$	$^3\text{He}$
Ca				
shift(cm <sup>-1</sup> )	203 <sup>b</sup>	112 <sup>b</sup>	72 <sup>a</sup>	–
FWHM(cm <sup>-1</sup> )	297 <sup>b</sup>	245 <sup>b</sup>	173 <sup>a</sup>	–
Sr				
shift(cm <sup>-1</sup> )	240 <sup>c</sup>	–	80	140
FWHM(cm <sup>-1</sup> )	287 <sup>c</sup>	–	180	220

<sup>a</sup> Ref. 17. <sup>b</sup> Ref. 20. <sup>c</sup> Ref. 39.

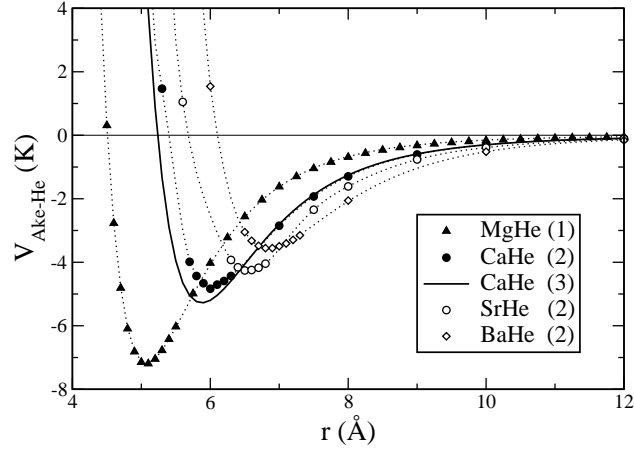


FIG. 1: Alkaline earth-He pair potentials used in this work to obtain the ground state structure of doped helium drops: (1) Ref. 30; (2) Ref. 29; (3) Ref. 32.

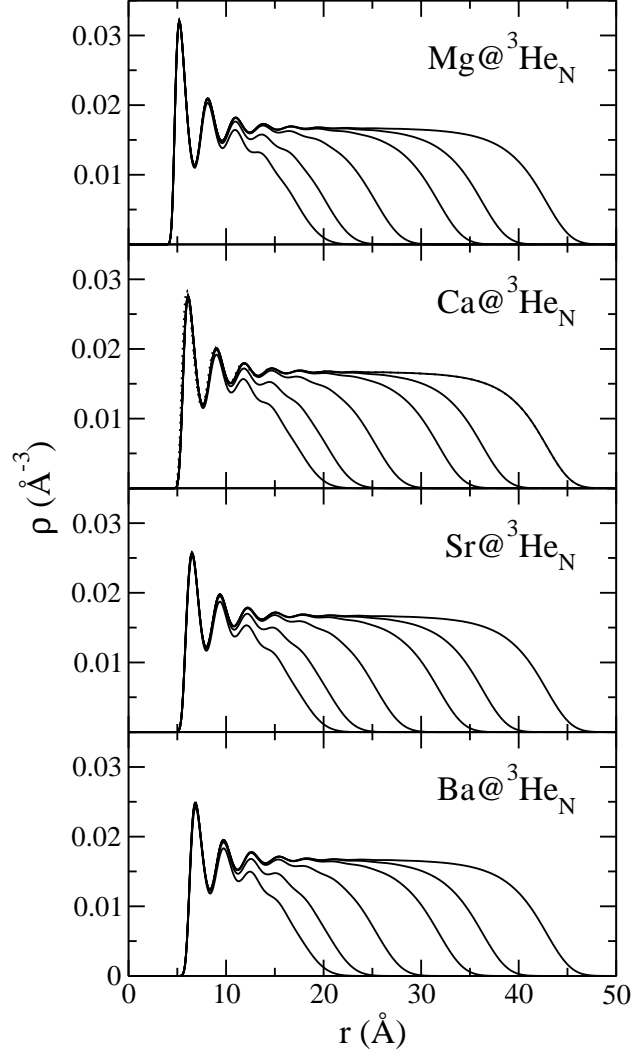


FIG. 2: Density profiles for  $^3\text{He}_N$  drops doped with Mg, Ca, Sr, and Ba, for  $N = 300, 500, 1000, 2000, 3000,$  and  $5000$ . The dotted line in the Ca panel corresponds to  $\text{Ca}@^3\text{He}_{5000}$  calculated with the pair potential of Ref. 32. Drops doped with Ca, Sr and Ba have been calculated using the pair potentials of Ref. 29, and drops doped with Mg, using the pair potential of Ref. 30.

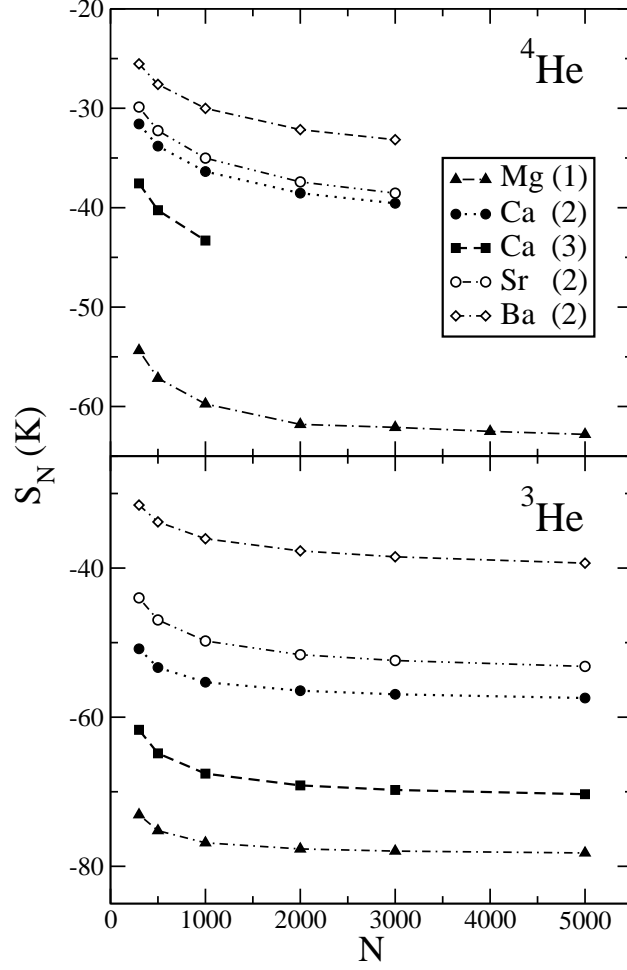


FIG. 3: Top panel: solvation energies (K) for doped  ${}^4\text{He}_N$  drops. Results obtained using the following pair potentials: (1) from Ref. 30; (2) from Ref. 29; (3) from Ref. 32. Bottom panel: same as top panel for doped  ${}^3\text{He}_N$  drops. The lines are drawn to guide the eye.



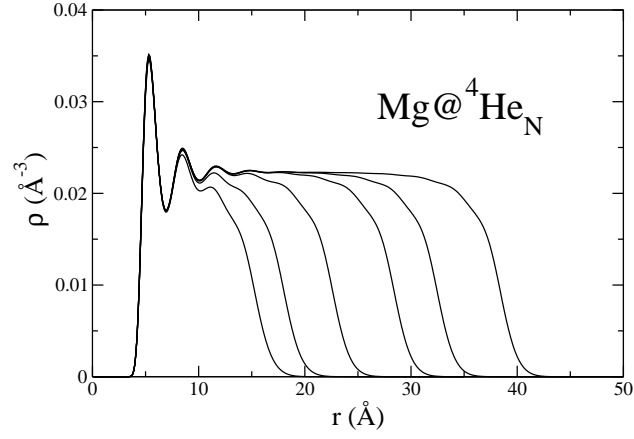


FIG. 4: Density profiles for  $\text{Mg}@^4\text{He}_N$  drops for  $N = 300, 500, 1000, 2000, 3000,$  and  $5000$ . Results obtained using the pair potential of Ref. 30.

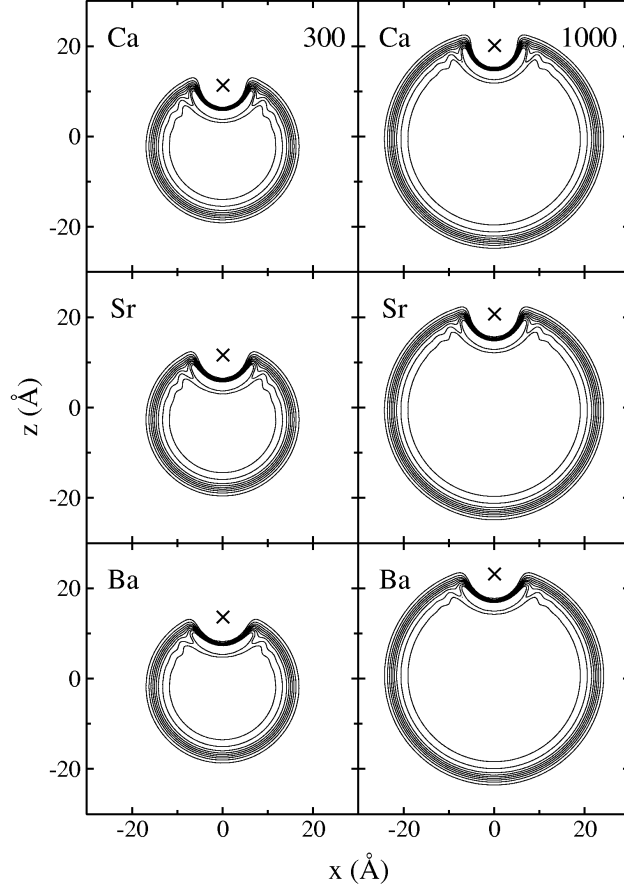


FIG. 5: Equidensity lines on a symmetry plane for  ${}^4\text{He}_N$  drops with  $N=300$  (left panels) and 1000 (right panels) doped with Ca, Sr and Ba. The lines span the surface region between  $0.9\rho_b$  and  $0.1\rho_b$  in  $0.1\rho_b$  steps, where  $\rho_b$  is the bulk liquid density  $0.0218 \text{ \AA}^{-3}$ . The cross indicates the location of the alkaline earth atom in the dimple. Results obtained using the pair potentials of Ref. 29.

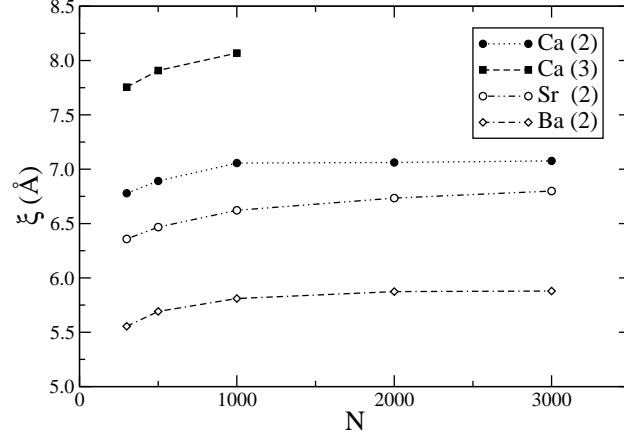


FIG. 6: Depth of the dimples ( $\xi$ ) created in  ${}^4\text{He}_N$  drops obtained using the following pair potentials: (2) from Ref. 29 for Ba (diamonds), Sr (circles), and Ca (solid dots) atoms; (3) from Ref. 32 for Ca (squares). The lines are drawn to guide the eye.

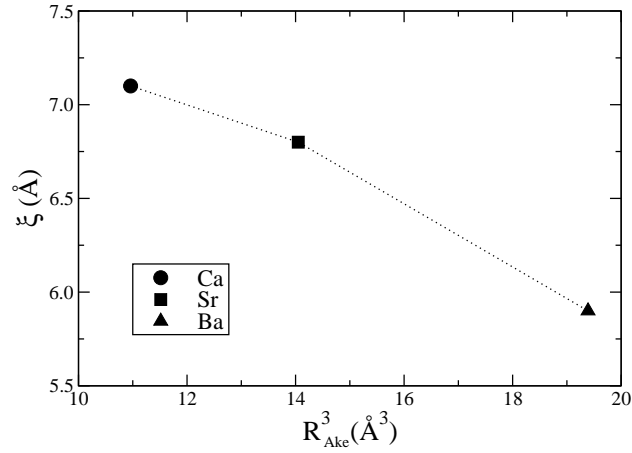


FIG. 7: Depth of the dimples ( $\xi$ ) created in  ${}^4\text{He}_{3000}$  drops by Ba, Sr and Ca atoms, as a function of the atomic size  $R_{Ake}^3$ , using the pair potentials of Ref. 29. The line is drawn to guide the eye.

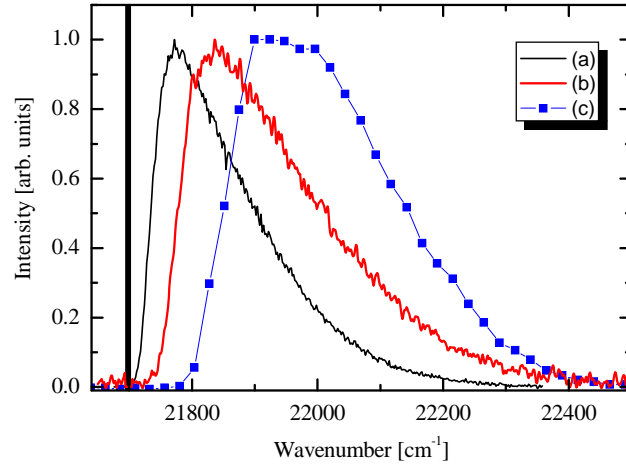


FIG. 8: Spectra of the Sr  $5s5p\ ^1P_1^o \leftarrow 5s^2\ ^1S_0$  transition: (a)  $^4\text{He}$  drops, (b)  $^3\text{He}$  drops, and (c) bulk  $^4\text{He}$ .<sup>39</sup> The vertical bar corresponds to the atomic line.